Deflagration-to-detonation transition in narrow channels: Hydraulic resistance vs. flame folding

L. Kagan and G. Sivashinsky
School of Mathematical Sciences, Sackler Faculty of Exact Sciences,
Tel Aviv University, Tel Aviv 69978, Israel

1 Abstract

This study is concerned with identification of the key interactions controlling deflagration-to-detonation transition (DDT) in narrow smooth-walled channels. Two agencies contributing to the transition are discussed: hydraulic resistance for very thin channels (thick flames) and flame folding for wider channels (moderately thick flames). The dual nature of the DDT mechanism is reflected in the non-monotinicity of the dependency of the run-up time/distance on the channel width.

2 Outline of the problem

Deflagration-to-detonation transition (DDT) occurring in smooth-walled thermally insulated channels, narrow enough to ensure the laminar character of the developing flow, is arguably the simplest system for theoretical/numerical exploration of the DDT. Yet, even under these benign conditions the emerging dynamical picture is complex enough [1-4] for straightforward identification of the mechanisms involved.

The present study is concerned with assessment of the relative impacts of hydraulic resistance and flame folding which have long been recognized as important players in the transition event [5-9].

To describe the DDT in a channel, a set of 2D Navier-Stokes equations for compressible reactive flows is employed; see Ref. [10] for details of equations and initial/boundary conditions. The reaction rate is modeled by a single-step second-order Arrhenius kinetics, $W = A\rho^2 C \exp(-E/RT)$, where ρ is the gas density, C is the mass fraction of the deficient reactant, and A is the Arrhenius prefactor.

Scaled variables and parameters appearing in the further discussion are defined as follows: Pr and Le are Prandtl and Lewis numbers; $Ma = u_p/a_p$, Mach number; u_p, velocity of the isobaric deflagration relative to the burned gas; $a_p = \sqrt{\gamma(c_p - c_v)T_p}$ sonic velocity at $T = T_p$; $T_p = T_0 + QC_0/c_p$, adiabatic temperature of burned gas (products) under constant pressure, $P = P_0$; T_0, initial temperature of unburned gas; Q, heat release; $\gamma = c_p/c_v$; c_p, c_v, specific heats; C_0, initial mass fraction of the deficient reactant; $(\hat{u}, \hat{v}) = (u, v)/a_p$, scaled flow velocity; $\hat{D} = D/a_p$, scaled reaction wave velocity; $(\hat{x}, \hat{y}) = (x, y)/x_p, \hat{t} = t/t_p$ scaled spatio-temporal coordinates; $x_p = a_p t_p; t_p = A^{-1} Z \exp(N_p)$, reference time; $N_p = E/RT_p$, scaled activation energy; $Z = \frac{1}{2} Le^{-1} N_p^2 (1 - \sigma_p)^2$, normalizing factor

Correspondence to: kaganleo@post.tau.ac.il

to ensure that at $N_p >> 1$ and isobaric conditions the scaled deflagration velocity relative to the burned gas is close to Ma; $\sigma_p = T_0/T_p$; $\hat{\rho} = \rho/\rho_p$, where $\rho_p = P_0/(c_p - c_v)T_p$ is the density of combustion products in isobaric deflagration; $\hat{W} = (t_p/\rho_p C_0)W$, scaled reaction rate; $x_p = a_p t_p = l_{th}/Ma$, where $l_{th} = D^p_{th}/u_p$; D^p_{th}, thermal diffusivity at $T = T_p$ and $P = P_0$; l_{th}, flame width scale; $\hat{d} = d/x_p = Ma(d/l_{th})$, scaled width of the channel.

3 Numerical simulations

The computational method adopted and its validation are discussed in Ref. [10]. Parameters employed are specified as follows,

$$Pr = 0.75, \quad Le = 1, \quad \gamma = 1.3, \quad N_p = 5, \quad \sigma_p = 0.125, \tag{1}$$

$$Ma = 0.05, \quad 0.05 < \hat{d} < 1 \ (1 < d/l_{th} < 20).$$

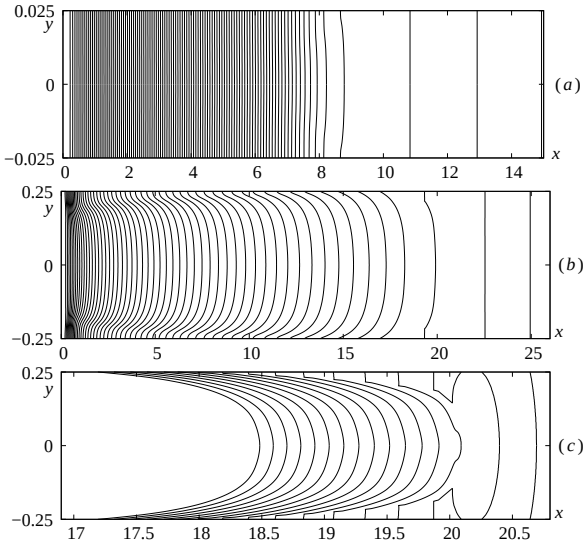

Figure 1: Reaction zone configurations ($\max \hat{W}$) at several equidistant instants of time calculated for $d = l_{th}$ (a) and $d = 10l_{th}$ $(b, c\text{-zoom})$. Note the disparity between the transverse and longitudinal scales: 45-fold (a), 20-fold (b) and 2.5-fold (c) compressions. The transition occurs in two stages - first near the wall and thereupon at the centerline, reflecting the dual nature of the transition event.

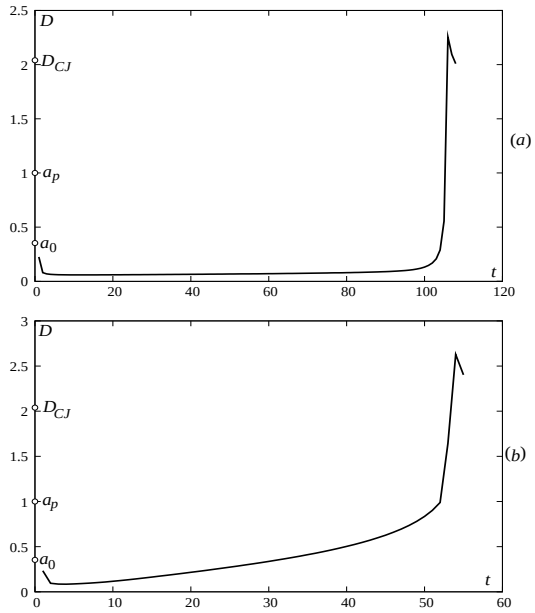

Figure 2: Time records of the reaction wave velocities $\hat{D}(\hat{t})$, calculated for $d = l_{th}$ (a) and $d = 10l_{th}$ (b) along the centreline $y = 0$. Here $\hat{D}_{CJ}$ corresponds to the Chapman-Jouguet detonation, and $\hat{a}_0$, $\hat{a}_p$ - to the sonic velocities in fresh and burned gas, respectively. In all the figures, the hats on the labels have been omitted.

Figures (1) (2) show the reaction zone configurations at several consecutive equidistant instants of time, and the time record of the reactive wave speed, calculated for $\hat{d} = 0.05$ $(d = l_{th})$ and $\hat{d} = 0.5$ $(d = 10l_{th})$. In both cases one observes the transition from deflagrative to detonative burning. However, at $d = l_{th}$ the transition occurs practically without the incipient acceleration, while at $d = 10l_{th}$ the acceleration is quite pronounced.

Flame folding and hydraulic resistance are invariably entangled through no-slip boundary conditions which makes a rational analysis of their individual influences very difficult. To assess the impact of

flame folding we calculated the gap $\hat{\delta}(\hat{t})$ between the leading and trailing parts of the advancing flame front, $\hat{x} = \hat{x}_f$,

$$\hat{\delta}(\hat{t}) = \max_{0<\hat{y}<\hat{d}} \hat{x}_f(\hat{y},\hat{t}) - \min_{0<\hat{y}<\hat{d}} \hat{x}_f(\hat{y},\hat{t}) \tag{2}$$

Figure (3) shows corresponding time records. Assuming the flame front to be parabolic (Figs. 1,2) we calculated the *degree of folding*,

$$\Sigma = \frac{flame\ front\ arclength}{channel\ width} = \tag{3}$$

$$\frac{1}{2}\left\{\sqrt{1+\left(\frac{4\hat{\delta}}{\hat{d}}\right)^2} + \left(\frac{\hat{d}}{4\hat{\delta}}\right)\ln\left[\frac{4\hat{\delta}}{\hat{d}} + \sqrt{1+\left(\frac{4\hat{\delta}}{\hat{d}}\right)^2}\right]\right\}$$

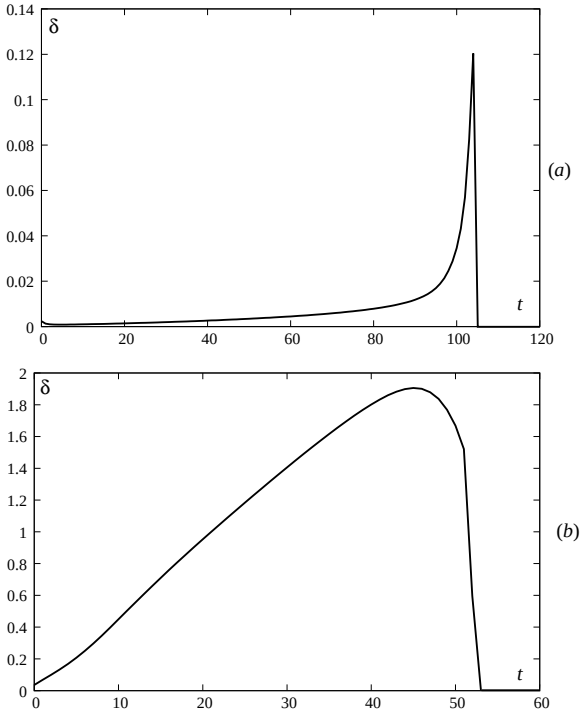

Figure 3: Time records of the reaction zone folding, $\hat{\delta} = \max \hat{x}_f(\hat{y}) - \min \hat{x}_f(\hat{y})$, calculated for $d = l_{th}$ (a) and $d = 10l_{th}$ (b).

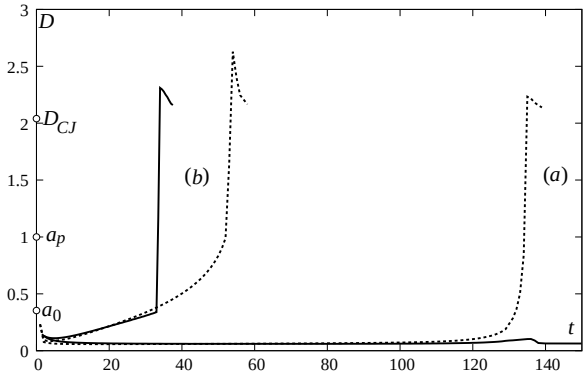

Figure 4: Time records of the reaction wave velocities $\hat{D}(\hat{t})$ for 1D Σ-models (solid lines) and for the associated 2D models (dashed lines), calculated for $d = 2l_{th}$ (a) and $d = 10l_{th}$ (b).

Then we considered a 1D *friction-free* version of the problem with the original reaction rate $\hat{W}$ replaced by,

$$\hat{W}_\Sigma = \Sigma^2 \hat{W}, \tag{4}$$

to ensure the overall mass flux through the flame $\hat{\rho}(\hat{D} - \hat{u})$ to be proportional to Σ.
For thick flames ($d = 2l_{th}$) the developing level of folding appears to be insufficient for triggering the transition (Fig. 4). However, for moderately thick flames ($d = 10l_{th}$) the transition indeed occurs, and even faster than in the original 2D model. The adopted 1D Σ-model therefore overestimates the folding effect and requires an appropriate mitigation. In any case, there appear to be two mechanisms capable of triggering the transition: hydraulic resistance for very thin channels and flame folding for wider channels.

Figure (5) depicts $\hat{D}$ vs. Σ dependency when Σ is considered as a prescribed time-independent parameter. Here, in line with the Deshais-Joulin positive feedback theory [5], the deflagrative burning is maintained only for sufficiently low Σ, converting abruptly into the CJ-detonation at $\Sigma > \Sigma_{DDT} = 6.1$.

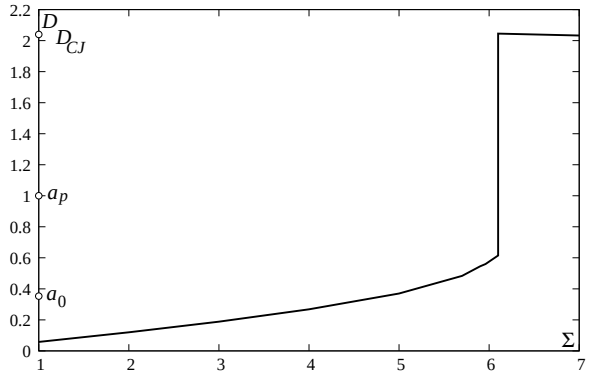

Figure 5: Reaction wave velocity $\hat{D}$ vs. degree of folding Σ, considered as a time-independent parameter.

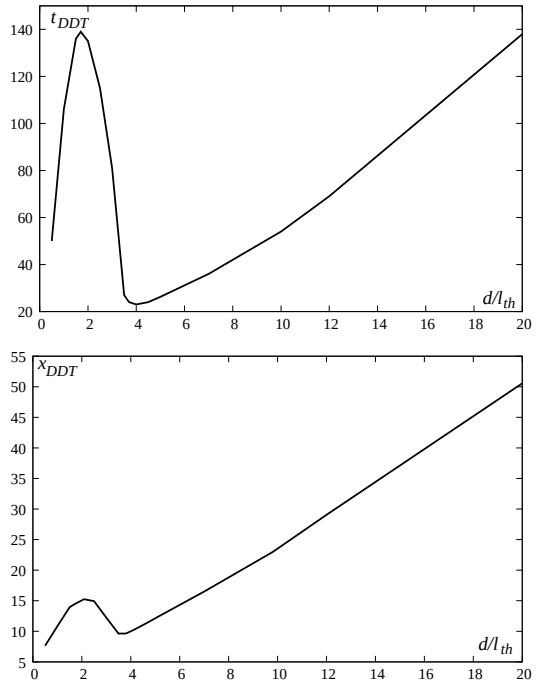

Figure 6: Run-up time ($\hat{t}_{DDT}$) and distance ($\hat{x}_{DDT}$) vs. normalized channel width d/l_{th}.

4 Non-monotinicity

There is a more direct indication of the possible change in the DDT mechanism. If one looks at the dependency of the run-up time ($\hat{t}_{DDT}$) and distance ($\hat{x}_{DDT}$) on the channel width, one observes a change of monotonicity at about $d = 2l_{th}$ (Fig. 6). At $d < 2l_{th}$ the flame folding is too mild and the transition is caused by the resistance induced precompression and preheating of the unburned gas adjacent to the advancing deflagration. The preheating eventually results in the thermal runaway (explosion) within the reaction zone, rendering further deflagrative propagation unsustainable [4]. The system is then compelled to find an alternative mode of dynamic equilibrium which is fast (subsonic or supersonic) compression-driven burning.

At $d < 2l_{th}$ the widening of the channel reduces the impact of hydraulic resistance thereby extending $\hat{t}_{DDT}$ and $\hat{x}_{DDT}$. A further widening of the channel ($d > 2l_{th}$) promotes the flame folding and hence the flame speed, causing reduction of $\hat{t}_{DDT}$ and $\hat{x}_{DDT}$. In this parameter range the flame-folding becomes an important influence invoking its own positive feedback mechanism of the transition, first described by Deshaies and Joulin [5]. And yet even further widening of the channel ($4l_{th} < d < 20l_{th}$) practically does not affect the final level of folding (Fig. 7), but merely slows down its formation, which results in the secondary buildup of the run-up time and distance (Fig. 6).

5 Prandtl number effect

For all the importance of the flame folding in wide channels and its ability to trigger DDT in unconfined voritcal flows ([5, 8], Fig. 5), in confined systems detonation generally nucleates in the boundary layer [11-13] (see also Fig. 1b,c) where the hydraulic resistance is known to promote the pressure buildup [10]. In theoretical analysis the level of hydraulic resistance may be altered by changing the Prandtl number, other conditions being fixed. Reduction of the Prandtl number extends the pre-detonation time (Fig. 8). This may be perceived as the influence of hydraulic resistance on the transition, although the impact of Prandtl number on the pre-detonation dynamics of flame-folding is likely also to be of consequence. More research on this intriguing issue is needed. A comprehensive yet tractable theory may be based on an autonomous quasi-one-dimensional model allowing for the flame folding and hydraulic resistance to act simultaneously.

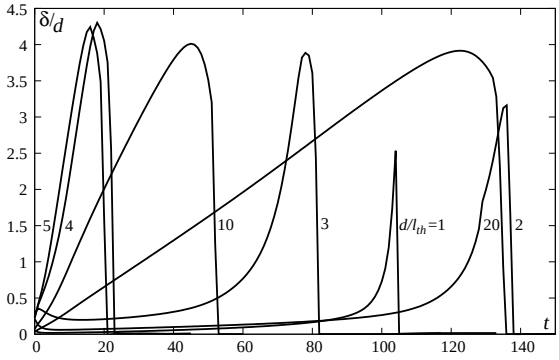

Figure 7: Time records of the normalized folding, $\hat{\delta}/\hat{d}$, calculated for several channel widths ($1 < d/l_{th} < 20$).

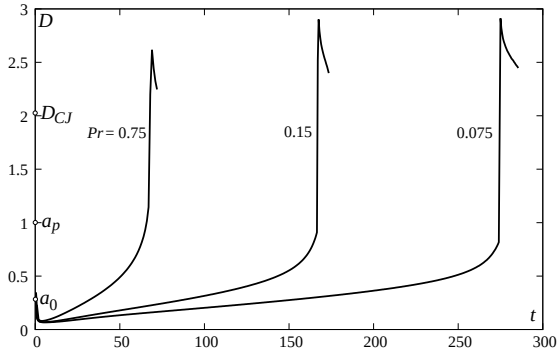

Figure 8: Time records of the reaction wave velocity $\hat{D}(\hat{t})$ calculated for $d = 12l_{th}$ at $Pr = 0.75, 0.15, 0.075$; other parameters as in Fig. 2.

6 Concluding remark

It would be desirable to test experimentally the found non-monotinicity effect, e.g. by extending recent studies of DDT in capillaries and sub-millimeter gaps [14-16] over *low-pressure* conditions – to facilitate formation of thick flames. Special care should be taken to reduce conductive heat losses whose influence increases for thick flames. Good insulation may presumably be attained in double walled vacuum ducts, or in an extended honeycomb-like arrangement with thin partitions - to reduce their impact on the gaseous phase.

Acknowledgments

These studies were supported in part by the US-Israel Binational Science Foundation (Grant 2012-057) and the Israel Science Foundation (Grant 335/13).

References

[1] J. Daou, M. Matalon, Influence of conductive heat-losses on the propagation of premixed flames in channels, *Combust. Flame* **128** (2002) 321-329.

[2] M. Short, D. A. Kessler, Asymptotic and numerical study of variable-density premixed flame propagation in a narrow channel. *J. Fluid Mech.* **638** (2009) 305-337.

[3] V. N. Kurdyumov, M. Matalon, Flame acceleration in long narrow open channels. *Proc. Combust. Inst.* **34** (2013) 865-872.

[4] L. Kagan, P. Gordon, G. Sivashinsky, An asymptotic study of the transition from slow to fast burning in narrow channels. *Proc. Combust. Inst.* **35** (2015) 913-920.

[5] B. Deshaies, G. Joulin, Flame-speed sensitivity to temperature changes and the deflagration-to-detonation transition. *Combust. Flame* **77** (1989) 201-212.

[6] V. Bychkov, A. Petchenko, V. Akkerman, L.-E. Erikson, Theory and modeling of accelerating flames in tubes. *Phys. Rev.* **E 72** (2005) 046307.

[7] E. S. Oran, V. N. Gamezo, Origins of the deflagration-to-detonation transition in gas-phase combustion. *Combust. Flame* **148** (2007) 4-47.

[8] A. Y. Poludnenko, T. A. Gardiner, E. S. Oran, Spontaneous transition of turbulent flames to detonations in unconfined media. *Phys. Rev. Lett.* **107** (2011) 054501.

[9] I. Brailovsky, L. Kagan, G. Sivashinsky, Combustion waves in hydraulically resisted systems. *Phil. Trans. R. Soc. A,* **370** (2012) 625-646.

[10] L. Kagan, G. Sivashinsky, The transition from deflagration to detonation in thin channels. *Combust. Flame* **134** (2003) 389-397.

[11] F. J. Martin, Transition from slow burning to detonation in gaseous explosives. *Phys. Fluids* **1** (1958) 399-407.

[12] P. A. Urtiew, A. K. Oppenheim, Experimental observations of the transition to detonation in an explosive gas. *Proc. R. Soc. Lond. A* **295** (1966) 13-28.

[13] M. Kuznetsov, V. Alekseev, I. Matsukov, S. Dorofeev, DDT in a smooth tube filled with a hydrogen/oxygen mixture. *Shock Waves* 14 (2005) 205-215.

[14] M.-H. Wu, M. P. Burke, F. Son, R. A. Yetter, Flame acceleration and the transition to detonation of stoichiometric ethylene/oxygen in microscale tubes. *Proc. Combust. Inst.* **31** (2007) 2429-2436.

[15] M.-H. Wu, C.-Y. Wang, Reaction propagation modes in millimeter-scale tubes for ethylene/oxygen mixtures *Proc. Combust. Inst.* **33** (2011) 2287-2293.

[16] M.-H. Wu, W.-C. Kuo, Accelerative expansion and DDT of stoichiometric ethylene/oxygen flame rings in micro-gaps. *Proc. Combust. Inst.* **34** (2013) 2017-2024.